

A new approach to parton recombination in a QCD evolution equation

Wei Zhu

Department of Physics, East China Normal University, Shanghai 200062, **P.R. China**

Abstract

Parton recombination is reconsidered in perturbation theory without using the AGK cutting rules in the leading order of the recombination. We use time-ordered perturbation theory to sum the cut diagrams, which are neglected in the GLR evolution equation. We present a set of new evolution equations including parton recombination.

1 Introduction

Parton recombination as a new higher twist phenomenon was first discussed in the QCD evolution process by Gribov, Levin, Ryskin [1] and Mueller, Qiu [2] in their pioneering works. This evolution equation is called the GLR equation.

An interesting effect of parton recombination is screening or shadowing. In the case of higher number densities of partons, for example in the small x region, the gluons can overlap spatially and annihilate. Therefore, one expects that the growth of the gluon density with Q^2 will be suppressed by gluon recombination. These suppression factors from the negative contributions due to gluon recombination are calculated in the GLR equation using the AGK (Abramovsky, Gribov, Kancheli) cutting rules [3]. Assuming that the AGK cutting rules are valid in deep inelastic scattering (DIS) in the small x region, one finds that the relative weights of cuts through two, one and zero ladders are $2 : -4 : 1$, as illustrated in fig. 1. Due to these quantitative predictions of the suppression of parton number densities at small x , the GLR equation was extensively used to explore the structure of the nucleon and new perturbative QCD (PQCD) effects in the past years.

However, the applications of AGK cutting rules in the GLR equation have some drawbacks. For example, the cut lines break the correlation between the recombining partons according to the AGK cutting rules in the GLR equation (fig. 1). As we will show in this work, the correlation among the initial partons in the QCD recombination equation should be preserved. On the other hand, two-to-two parton processes may be associated with IR-divergences just as are the one-to-two processes in the Dokshitzer-Gribov-Lipatov-Altarelli-Parisi (DGLAP) evolution equation [4-6]. Although the AGK cutting rules provide simple relations between the cross sections of hadron-hadron interactions for different types of reggeon cuts, however, the sum of cut graphs according to the AGK cutting rules cannot cancel IR-divergences. The reason is that the difference of the contributions between the positive graph and the negative graph is only a weight, according to the AGK cutting rules. As we know that the virtual diagrams are necessary for cancellation of IR-divergences in the DGLAP equation. We will show in this work that above mentioned IR-divergences in two-to-two processes also can be canceled by the sum of virtual diagrams, which are neglected in the GLR equation.

In this work, we reconsider parton recombination in the QCD evolution equation without the AGK cutting rules. To this end, we first point out that a new scale (the recombination scale) exists in the parton recombination processes. We will give a definition of the recombination order of the process. Then, we propose the bare probe-vertex approximation. We find that several more diagrams, which are neglected in the GLR equation, should be included in the QCD equation of the parton fusion. We try to find a simple way to calculate those cut diagrams in time-ordered perturbation theory (TOPT). Through a new derivation of the DGLAP evolution equation, we present simple connections among the different cut diagrams. We shall show that both the shadowing-antishadowing and momentum conservation are the natural results of the theory. As an interesting result, our new equation has different structure from the GLR equation.

The outline of the paper is the following. In section 2 we give some definitions related to the parton model. In section 3 the sum of the cut diagrams at the bare probe-vertex approximation is proposed. In section 4 we give a new derivation of the DGLAP equation.

Through this example, we try to show the connections among the relative cut graphs at the leading recombination order. The new evolution equations incorporating the parton recombination are derived in sections 5–7. Section 8 contains the discussions and concluding remarks.

2 Definitions

According to PQCD, a parton can always independently split into two partons. However, except in the PQCD dynamics, the recombination of partons depends on the overlap probability of their wave functions. Therefore, we need a new physical quality to characterize parton recombination.

For example, consider an amplitude with two initial partons. According to dimensional analysis, the hadronic part of the amplitude should contain a factor $\sim 1/R$, where R has dimension of length. Now we incorporate the factor $1/Q$ arising from the partonic part of the amplitude to form a dimensionless quality $1/(RQ)$. We call this the recombination factor. For example, the recombination factor of the process with two initial correlated partons is $1/(RQ)^2$. One can schematically think of $1/(RQ)^2$ as the overlap probability of two partons, where $1/Q$ is the scale of a parton at momentum transfer Q^2 and R is the maximum correlation length of two partons. Usually, R is regarded as the scale of target or the scale of the “hot spots”, if they exist in the proton. This definition can be generalized to the case of the amplitudes including m -initial partons; the recombination factor in this case is $1/(RQ)^{m-1}$ if the fusing partons are paired.

In this paper, we consider only the recombination processes at the leading order level, that is, at $1/(RQ)^2$ and α_s^2 . Therefore, we choose to study the following basic amplitudes as shown in fig. 2: (a) $M_{p\gamma^* \rightarrow k'l'X}^{(2-1)}$, (b) $M_{p\gamma^* \rightarrow k'l'X}^{(2-2)}$ and (c) $M_{p\gamma^* \rightarrow k'l'X}^{(2-3)}$, with the recombination factors $1/(RQ)^0$, $1/(RQ)^1$ and $1/(RQ)^2$, respectively. In fig. 2 we have omitted the distinction of the parton flavors; the dark circles indicate QCD interactions among the correlating partons.

We see that the amplitudes involving parton recombination contain the double scales: $1/(RQ)$ and α_s . We shall perform the calculations at a given order- $1/(RQ)^m$ and order- $(\alpha_s)^n$ in two steps. First, we calculate the process at the order of $1/(RQ)^2$. In this case, the dark circles in fig. 2 are regarded as the elemental sub-processes. The reason is that the decomposition of the circle part will break the parton correlation and reduce the order of the recombination. The second step is to calculate the sub-processes at order- α_s^2 in PQCD.

We will use TOPT in this work. Usually, TOPT is equivalent to the standard covariant perturbation theory [7]. We shall call this TOPT as the normal TOPT (NTOPT), where the time lines divide every basic vertex along the time-order. In TOPT, the internal lines and the virtual particles are expressed by external lines and effective real particles respectively. Therefore, TOPT can also be used to describe amplitudes involving complex vertices, where the part between two neighboring time lines can contain a complex vertex. We define such a TOPT as an anomalous TOPT (ATOPT). Obviously, ATOPT is not equivalent to NTOPT: they have different energy deficits. On the other hand, there are energy-momentum correlation between two neighboring complex vertices in ATOPT; therefore, the vertex in ATOPT is not really factorized.

We take the physical axial gauge, where the light-like vector n fixes the gauge as $n \cdot A = 0$, A being the gluon field. The parton number densities are defined within the parton model description of the photon nucleon DIS (fig. 3a) as

$$d\sigma(\gamma^* p \rightarrow k' X) = \int dx_1 q(x_1) d\sigma(\gamma^* k \rightarrow k'), \quad (2.1)$$

where $q(x_1)dx_1$ is the number of quarks carrying momentum fraction between x_1 and $x_1 + dx_1$, where $x_1 = k \cdot n / p \cdot n$. Formula (2.1) means that the interaction of a virtual photon with proton can be factorized as the soft part $q(x_1)$ and hard part $d\sigma(\gamma^* k \rightarrow k')$. According to the parton model,

$$d\sigma(\gamma^* k \rightarrow k') = C_q \delta(x_1 - x_B), \quad (2.2)$$

where $x_B = Q^2/2p \cdot q$ and C_q is the coefficient depending on x_B and Q^2 . The quark density can be defined as

$$q(x_B) = \frac{1}{C_q} d\sigma(\gamma^* p \rightarrow k' X). \quad (2.3)$$

On the other hand, using TOPT in the cut graph 3b, we have

$$\begin{aligned} & d\sigma(\gamma^* p \rightarrow k' X) \\ &= \frac{E_k}{E_p} |M_{p \rightarrow kX}|^2 \left[\frac{1}{E_p - E_k - E_X} \right]^2 \left[\frac{1}{2E_k} \right]^2 \prod_X \frac{d^3 k_X}{(2\pi)^3 2E_X} \\ & \quad \frac{1}{8E_k E_\gamma} |M_{\gamma^* k \rightarrow k'}|^2 (2\pi)^4 \delta^4(p_\gamma + k - k') \frac{d^3 k'}{(2\pi)^3 2E_{k'}}. \end{aligned} \quad (2.4)$$

Comparing eqs. (2.1) with (2.4), we get the definitions of the quark number density

$$\begin{aligned} & q(x_1)dx_1 \\ &= \frac{E_k}{E_p} |M_{p \rightarrow kX}|^2 \left[\frac{1}{E_p - E_k - E_x} \right]^2 \left[\frac{1}{2E_k} \right]^2 \prod_X \frac{d^3 k_X}{(2\pi)^3 2E_X}. \end{aligned} \quad (2.5)$$

and the bare probe-parton vertex

$$\begin{aligned} & \frac{1}{C_q} d\sigma(\gamma^* k \rightarrow k') \\ &= \frac{1}{C_q} \frac{1}{8E_k E_\gamma} |M_{\gamma^* k \rightarrow k'}|^2 (2\pi)^4 \delta^4(p_\gamma + k - k') \frac{d^3 k'}{(2\pi)^3 2E_{k'}} \\ &= \delta(x_1 - x_B), \end{aligned} \quad (2.6)$$

in the TOPT-form.

3 Bare probe-vertex approximation

As we know, emission or absorption of quanta with zero-momentum may associate with the infrared (IR) divergence. However, the singular terms provide the leading contributions to the DIS processes. Therefore, a correct theory is IR-safe, where IR-divergences are canceled, while the leading contributions are retained. One way can to attain above two goals is to sum over cut diagrams belonging to the same time-ordered uncut graph, since these graphs have similar singular structure but may come up with opposite signs.

Deep inelastic scattering structure functions are the imaginary parts of the amplitudes for the forward ‘Compton’ scattering of the target with a probe. Using the time-ordered perturbative expansion of the statement of the unitarity of the S-matrix, one can prove that the structure functions are associated with the sum of cut diagrams. These different cut graphs represent various possible sub-partonic processes due to the unitarity of the perturbative S-matrix [7]. Therefore, the sum of cut graphs is necessary not only for infrared safety, but also for collecting the leading contributions and restoring the unitarity.

The interesting and important question is, what are the minimum cut diagrams that must be summed for IR-safe calculation of an inclusive DIS process at a given order (for example, order $\alpha_s^2/(RQ)^2$ in this work) ?

To answer this question, let us consider a general inclusive DIS process on target N. One can choose the cut diagrams according to following program: $G(N)$ stands for the time-ordered uncut diagram of the target N without probe vertices. We sum over possible cut diagrams of $G(N)$:

$$\sum_{\gamma} G_{\gamma}(N) = \{\sum_{\gamma} L_{\gamma} R_{\gamma}\}_I, \quad (3.1)$$

where G_{γ} is the cut diagram with cut line γ ; L_{γ} and R_{γ} are the sub-graphs on the left and right of the cut line; the subscript “I” means that we only consider following cut graphs which have the same observed quantities (that is, the same structure of the intermediate state) and which keep the original correlation among initial partons in $G(N)$.

We use the probe to observe the parton distributions inside the target in DIS. Of course, we cannot control the probing positions. In principle, in- and out-probe lines can be attached to the left- and right-hand of the cut line in all possible ways. Let $G_{\gamma}^{\beta}(probe + N)$ stand for the cut diagrams of the probe-target system, where β labels the probe-parton vertices. Thus, we shall sum over

$$\sum_{\beta} \sum_{\gamma} G_{\gamma}^{\beta}(probe + N). \quad (3.2)$$

Obviously, the sum (3.2) is much larger than $\sum_{\gamma} G_{\gamma}(N)$. Now we try to find some approximation in the sum (3.2). As we know that the leading logarithmic approximation (LLA) is a good approximation for IR-safeness in the DGLAP equation at order- α_s . In this approximation, some of the renormalization effects are neglected in the physical gauge and the probe-vertex retains the bare-vertex form as in (2.6). In this case,

$$G_{\gamma}^{\beta}(probe + N) = G_{\gamma}(N) \delta(x_{\gamma} - x_B), \quad (3.3)$$

Thus, the contributions from the nonlocal interactions of probe with partons are neglected at the leading approximation. We need only to sum part of cut graphs, in which the bare-probe vertex $\delta(x_\gamma - x_B)$ connects with the cut line, that is,

$$\begin{aligned}
& \sum_{\beta} \sum_{\gamma} G_{\gamma}^{\beta}(\text{probe} + N) \\
&= \sum_{\gamma} G_{\gamma}(N) \delta(x_{\gamma} - x_B) \\
&= \sum_{\gamma} \{L_{\gamma} R_{\gamma}\}_I \delta(x_{\gamma} - x_B),
\end{aligned} \tag{3.4}$$

in the DIS processes with parton recombination.

We call (3.4) as the bare probe-vertex approximation. We find that this approximation is also a satisfactory approximation in the DIS processes with parton recombination. In fact, our interest is that the modifications of the parton recombination to the DGLAP equation, which has the probability explanation at the LLA approximation. We shall show that the bare probe-vertex approximation is necessary for keeping the probability picture of the new evolution equation.

4 Rederivation of the DGLAP equation

We know that several methods can be used to derive the DGLAP evolution equations, however, the following new method illustrates more clearly the simple relations among the cut diagrams in the sum (3.4). For simplicity, we only consider the non-singlet case. According to (3.4) we compute fig. 4a with figs. 4b and 4c. Figures 4b and 4c seem to change the observed quantity $d \ln l_{\perp}^2$, where l_{\perp} is the transverse momentum of the final state partons, (see fig. 2a) whose momenta are parametrized as

$$\begin{aligned}
l &= [x_1 p, \underline{0}, x_1 p], \\
k &= \left[x_2 p + \frac{l_{\perp}^2}{2x_2 p}, l_{\perp}, x_2 p \right], \\
l' &= \left[x_3 p + \frac{l_{\perp}^2}{2x_3 p}, -l_{\perp}, x_3 p \right].
\end{aligned} \tag{4.1}$$

However, we will see that the contribution of an intermediate state can be replaced by $d^3 l'$, which is from the contribution of the loop and contributes $d \ln l_{\perp}^2$. Therefore, all the processes of fig. 4 have the same intermediate state structure.

We proceed along the lines of ref.[8]. The change of the valence-quark-number density caused by gluon radiation can be written as (see fig. 4a)

$$\begin{aligned}
dq(x_B) &= \frac{1}{C_q} d\sigma(\gamma^* p \rightarrow k' X) \\
&= \frac{E_l}{E_p} |M_{p \rightarrow lX}|^2 \left[\frac{1}{E_p - E_l - E_X} \right]^2 \left[\frac{1}{2E_l} \right]^2 \prod_X \frac{d^3 k_X}{(2\pi)^3 2E_X}
\end{aligned}$$

$$H(\gamma^* l \rightarrow \gamma^* l), \quad (4.2)$$

where the cross section is factorized to the soft part and the hard part $H(\gamma^* l \rightarrow \gamma^* l)$ according to the factorization theory [9,10]. Using TOPT we obtain the hard part

$$\begin{aligned} & H(\gamma^* l \rightarrow \gamma^* l) \\ &= \frac{1}{C_q} \frac{1}{8E_k E_\gamma} |M_{\gamma^* k \rightarrow k'}|^2 (2\pi)^4 \delta^4(p_\gamma + k - k') \frac{d^3 k'}{(2\pi)^3 2E_{k'}} \\ & \quad \frac{E_k}{E_l} |M_{l \rightarrow k l'}|^2 \left[\frac{1}{E_l - E_k - E_{l'}} \right]^2 \left[\frac{1}{2E_k} \right]^2 \frac{d^3 l'}{(2\pi)^3 2E_{l'}}. \end{aligned} \quad (4.3)$$

Assuming that $l_\perp^2 \sim Q^2$, we have

$$\begin{aligned} & \frac{dq(x_B, Q^2)}{d \ln Q^2} \\ &= \int q(x_1, Q^2) P_2^{qq}(x_1, x_2, x_3) \delta(x_1 - x_2 - x_3) \delta(x_2 - x_B) dx_1 dx_2 dx_3 \\ &= \int q(x_1, Q^2) P_2^{qq}(z) dz \delta(x_1 z - x_B) dx_1 \\ &= \int q(x_1, Q^2) P_2^{qq}\left(\frac{x_B}{x_1}\right) \frac{dx_1}{x_1}, \end{aligned} \quad (4.4)$$

where

$$q(x_1, Q^2) dx_1 = \frac{E_l}{E_p} |M_{p \rightarrow l X}|^2 \left[\frac{1}{E_p - E_l - E_X} \right]^2 \left[\frac{1}{2E_l} \right]^2 \prod_X \frac{d^3 k_X}{(2\pi)^3 2E_X}, \quad (4.5)$$

as same as eq.(2.5) and

$$\delta(x_2 - x_B) = \frac{1}{C_q} \frac{1}{8E_k E_\gamma} |M_{\gamma^* k \rightarrow k'}|^2 (2\pi)^4 \delta^4(p_\gamma + k - k') \frac{d^3 k'}{(2\pi)^3 2E_{k'}}. \quad (4.6)$$

In eq.(4.4) we inserted

$$\int \delta(x_1 - x_2 - x_3) dx_2 = 1. \quad (4.7)$$

We define

$$P_2^{qq}(x_1, x_2, x_3) dx_3 \frac{dl_\perp^2}{l_\perp^2} = \frac{E_k}{E_l} |M_{l \rightarrow k l'}|^2 \left[\frac{1}{E_l - E_k - E_{l'}} \right]^2 \left[\frac{1}{2E_k} \right]^2 \frac{d^3 l'}{(2\pi)^3 2E_{l'}}, \quad (4.8)$$

as the parton splitting function for the non-singlet part.

Now let us consider figs. 4b and 4c. As for the the real diagram, the contributions of fig. 4b to the change of the valence-quark-number density are

$$\begin{aligned} dq(x_B) &= \frac{1}{2} \frac{1}{C_q} d\sigma(\gamma^* p \rightarrow k' X) \\ &= \frac{1}{2} \frac{E_l}{E_p} |M_{p \rightarrow l X}|^2 \left[\frac{1}{E_p - E_l - E_X} \right]^2 \left[\frac{1}{2E_l} \right]^2 \prod_X \frac{d^3 k_X}{(2\pi)^3 2E_X} \end{aligned}$$

$$H(\gamma^*l \rightarrow \gamma^*l), \quad (4.9)$$

where the factor of $\frac{1}{2}$ was explained as the effect of the renormalization in ref. [11]: The virtual part of fig.4b corresponds to the renormalization of a parton propagator. Only half of the probe-vertex connects with this parton line. This is equivalent to multiplying the virtual process by an extra factor of $\frac{1}{2}$.

The hard part in eq.(4.9) is

$$\begin{aligned} & H(\gamma^*l \rightarrow \gamma^*l) \\ &= \frac{1}{C_q} \frac{1}{8E_l E_\gamma} |M_{\gamma^*l \rightarrow k'}|^2 (2\pi)^4 \delta^4(p_\gamma + l - k') \frac{d^3 k'}{(2\pi)^3 2E_{k'}} \\ & \frac{d^3 l'}{(2\pi)^3} M_{l \rightarrow k l'} \frac{1}{2E_k} \frac{1}{2E_{l'}} \frac{1}{E_l - E_k - E_{l'}} M_{k l' \rightarrow l} \frac{1}{E_k + E_{l'} - E_l} \frac{1}{2E_l} \\ &= -\frac{1}{C_q} \frac{1}{8E_l E_\gamma} |M_{\gamma^*l \rightarrow k'}|^2 (2\pi)^4 \delta^4(p_\gamma + l - k') \frac{d^3 k'}{(2\pi)^3 2E_{k'}} \\ & \frac{E_k}{E_l} |M_{l \rightarrow k l'}|^2 \left[\frac{1}{E_l - E_k - E_{l'}} \right]^2 \left[\frac{1}{2E_k} \right]^2 \frac{d^3 l'}{(2\pi)^3 2E_{l'}}. \end{aligned} \quad (4.10)$$

Therefore we have

$$\begin{aligned} & \frac{dq(x_B, Q^2)}{d \ln Q^2} \\ &= - \int \frac{1}{2} q(x_1, Q^2) P_2^{qq}(x_1, x_2, x_3) \delta(x_1 - x_2 - x_3) \delta(x_1 - x_B) dx_1 dx_2 dx_3 \\ &= - \int \frac{1}{2} q(x_1, Q^2) P_2^{qq}(z) dz \delta(x_1 - x_B) dx_1 \\ &= -\frac{1}{2} q(x_B, Q^2) \int P_2^{qq}(z) dz, \end{aligned} \quad (4.11)$$

in which we have used eqs.(2.5),(2.6) and (4.8).

The contributions of fig. 4c is same as one of fig. 4b. Thus, the total contributions of the real- and virtual-diagrams are

$$\frac{dq(x_B, Q^2)}{d \ln Q^2} = \int q(x_1, Q^2) P_2^{qq}\left(\frac{x_B}{x_1}\right) \frac{dx_1}{x_1} - q(x_B, Q^2) \int P_2^{qq}(z) dz, \quad (4.12)$$

in which

$$P_2^{qq}(z) = \frac{\alpha_s}{2\pi} C_2(R) \frac{1+z^2}{1-z}. \quad (4.13)$$

The two terms of the right-hand side in eq.(4.12) have a simple interpretation: the positive contribution arises from the splitting of higher momentum quarks, while the negative contribution results in the loss of the number of quarks due to its gluon radiation.

The result (4.12) is the same as the probability form of the DGLAP equation for the nonsinglet part in ref. [11]. However, the new derivation clearly shows the following interesting properties in the inclusive DIS processes: The contributions of the cut diagrams,

which belong to a same time-ordered uncut graph in the sum (3.4), have an identical integral kernel (it is the parton splitting function in eq.(4.12)). This is a reason we use the TOPT form to perform our calculations. We shall examine this connection further in the parton recombination processes.

5 Leading recombination approximation

So far we considered processes contributing to the usual DGLAP equation. We go on now to include parton recombination processes. The recombination processes contributing at leading order come from the terms, $|M_{p\gamma^* \rightarrow k'l'X}^{(2-2)}|^2$, $2M_{p\gamma^* \rightarrow k'l'X}^{(2-1)}[M_{p\gamma^* \rightarrow k'l'X}^{(2-3)}]^*$, and the cut diagrams according to (3.4).

In this section we regard the partons as scalar particles (i.e., the ϕ^3 model). The results can easily be generalized to the case of QCD partons and will be done later in section 7. We consider the process of fig. 5, where figs. 5c–f are virtual. The contribution of the real diagram fig. 5a is

$$\begin{aligned} d\phi(x_B) &= \frac{1}{C_\phi} d\sigma(\gamma^* p \rightarrow k' X) \\ &= \frac{\sqrt{E_{p_1} + E_{p_2}} \sqrt{E_{p'_1} + E_{p'_2}}}{E_p} M_{p \rightarrow p_1 p_2 X} [M_{p \rightarrow p'_1 p'_2 X}]^* \\ &\quad \left(\frac{1}{E_p - E_{p_1} - E_{p_2} - E_X} \right)^2 \frac{1}{2E_{p_1}} \frac{1}{2E_{p_2}} \frac{1}{2E_{p'_1}} \frac{1}{2E_{p'_2}} \prod_X \frac{d^3 k_X}{(2\pi)^3 2E_X} \\ &\quad H(\gamma^* p_1 p_2 \rightarrow \gamma^* p'_1 p'_2), \end{aligned} \quad (5.1)$$

where C_ϕ is defined by

$$d\sigma(\gamma^* k \rightarrow k') = C_\phi \delta(x_1 - x_B), \quad (5.2)$$

for the scalar parton; the hard part is given by,

$$\begin{aligned} &H(\gamma^* p_1 p_2 \rightarrow \gamma^* p'_1 p'_2) \\ &= \left(\frac{1}{R} \right)^2 \frac{1}{C_\phi} \frac{1}{8E_k E_\gamma} |M_{\gamma^* k \rightarrow k'}|^2 (2\pi)^4 \delta^4(p_\gamma + k - k') \frac{d^3 k'}{(2\pi)^3 2E_{k'}} \\ &\quad \frac{E_k}{\sqrt{E_{p_1} + E_{p_2}} \sqrt{E_{p'_1} + E_{p'_2}}} M_{p_1 p_2 \rightarrow k l'} [M_{p'_1 p'_2 \rightarrow k l'}]^* \left(\frac{1}{E_{p_1} + E_{p_2} - E_k - E_{l'}} \right)^2 \\ &\quad \left(\frac{1}{2E_k} \right)^2 \frac{d^3 l'}{(2\pi)^3 2E_{l'}}. \end{aligned} \quad (5.3)$$

We define the parton correlation function (PCF) $f(x_1, x_2; x'_1, x'_2)$ as [12],

$$f(x_1, x_2; x'_1, x'_2) \delta(x_1 + x_2 - x'_1 - x'_2) dx_1 dx'_1 dx_2 dx'_2$$

$$\begin{aligned}
&= \frac{\sqrt{E_{p_1} + E_{p_2}} \sqrt{E_{p'_1} + E_{p'_2}}}{E_p} M_{p \rightarrow p_1 p_2 X} [M_{p \rightarrow p'_1 p'_2 X}]^* \left(\frac{1}{E_p - E_{p_1} - E_{p_2} - E_X} \right)^2 \\
&\quad \frac{1}{2E_{p_1}} \frac{1}{2E_{p_2}} \frac{1}{2E_{p'_1}} \frac{1}{2E_{p'_2}} \prod_X \frac{d^3 k_X}{(2\pi)^3 2E_X}, \tag{5.4}
\end{aligned}$$

while the parton recombination function $P_4^{(2-2)}$ is defined by

$$\begin{aligned}
&P_4^{(2-2)}(x_1, x_2, x'_1, x'_2, x_3, x_4) dx_4 \frac{dl_\perp^2}{l_\perp^4} \\
&= \frac{E_k}{\sqrt{E_{p_1} + E_{p_2}} \sqrt{E_{p'_1} + E_{p'_2}}} M_{p_1 p_2 \rightarrow k l'} [M_{p'_1 p'_2 \rightarrow k l'}]^* \left(\frac{1}{E_{p_1} + E_{p_2} - E_k - E_{l'}} \right)^2 \\
&\quad \left(\frac{1}{2E_k} \right)^2 \frac{d^3 l'}{(2\pi)^3 2E_{l'}}. \tag{5.5}
\end{aligned}$$

We shall discuss the PCF and the parton recombination function in sections 6 and 7, respectively. Therefore, we have

$$\begin{aligned}
&\frac{d\phi(x_B, Q^2)}{d \ln Q^2} \\
&= \left(\frac{1}{RQ} \right)^2 \int f(x_1, x_2, x'_1, x'_2, Q^2) \delta(x_1 + x_2 - x'_1 - x'_2) P_4^{(2-2)}(x_1, x_2, x'_1, x'_2, x_3, x_4) \\
&\quad \delta(x_3 - x_B) \delta(x_1 + x_2 - x_3 - x_4) dx_1 dx_2 dx'_1 dx'_2 dx_3 dx_4, \tag{5.6}
\end{aligned}$$

We shall discuss the PCF and the parton recombination function in sections 6 and 7, respectively. Therefore, we have

$$\begin{aligned}
&\frac{dq(x_B, Q^2)}{d \ln Q^2} \\
&= \left(\frac{1}{RQ} \right)^2 \int f(x_1, x_2, x'_1, x'_2, Q^2) \delta(x_1 + x_2 - x'_1 - x'_2) P_4^{(2-2)}(x_1, x_2, x'_1, x'_2, x_3, x_4) \\
&\quad \delta(x_3 - x_B) \delta(x_1 + x_2 - x_3 - x_4) dx_1 dx_2 dx'_1 dx'_2 dx_3 dx_4, \tag{5.5}
\end{aligned}$$

where we have inserted a factor $1 = \int \delta(x_1 + x_2 - x_3 - x_4) dx_3$. This is the evolution equation from fig. 5a.

Similarly, using the factorization in DIS [9,10], the contribution of fig. 5c (virtual diagram) is

$$\begin{aligned}
d\phi(x_B) &= \frac{1}{2} \frac{1}{C_\phi} d\sigma(\gamma^* p \rightarrow k' X) \\
&= \frac{1}{2} \frac{\sqrt{E_{p_1} + E_{p_2}} \sqrt{E_{p'_1} + E_{p'_2}}}{E_p} M_{p \rightarrow p_1 X} [M_{p \rightarrow p'_1 p'_2 p_2 X}]^* \\
&\quad \frac{1}{E_p - E_{p_1} - E_X} \left(\frac{1}{E_p - E_{p'_1} - E_{p'_2} - E_{p_2} - E_X} \right)^* \frac{1}{2E_{p_1}} \frac{1}{2E_{p_2}} \frac{1}{2E_{p'_1}} \frac{1}{2E_{p'_2}} \prod_X \frac{d^3 k_X}{(2\pi)^3 2E_X}
\end{aligned}$$

$$H(\gamma^* p_1 p_2 \rightarrow \gamma^* p'_1 p'_2). \quad (5.7)$$

Now the PCF is defined by

$$\begin{aligned} & f(x_1; x_2, x'_1, x'_2) dx_1 dx'_1 dx_2 dx'_2 \\ &= \frac{\sqrt{E_{p_1} + E_{p_2}} \sqrt{E_{p'_1} + E_{p'_2}}}{E_p} M_{p \rightarrow p_1 X} [M_{p \rightarrow p'_1 p'_2 p_2 X}]^* \\ & \frac{1}{E_p - E_{p_1} - E_X} \left(\frac{1}{E_p - E_{p'_1} - E_{p'_2} - E_{p_2} - E_X} \right)^* \\ & \frac{1}{2E_{p_1}} \frac{1}{2E_{p_2}} \frac{1}{2E_{p'_1}} \frac{1}{2E_{p'_2}} \prod_X \frac{d^3 k_X}{(2\pi)^3 2E_X}. \end{aligned} \quad (5.8)$$

However, we have the condition,

$$f(x_1; x_2, x'_1, x'_2) = f(x_1, x_2; x'_1, x'_2), \quad (5.9)$$

since the PCFs with cuts at different places are the same on the light-cone (fig.6) [13,14].

The hard part is given by

$$\begin{aligned} & H(\gamma^* p_1 p_2 \rightarrow \gamma^* p'_1 p'_2) \\ &= \left(\frac{1}{R}\right)^2 \frac{1}{C_\phi} \frac{1}{8E_\gamma} |M_{\gamma^* p_1 \rightarrow k'}|^2 (2\pi)^4 \delta^4(p_\gamma + p_1 - k') \frac{d^3 k'}{(2\pi)^3 2E_{k'}} \\ & \frac{1}{\sqrt{E_{p_1} + E_{p_2}} \sqrt{E_{p'_1} + E_{p'_2}}} \frac{1}{2E_{p_1}} \frac{d^3 l'}{(2\pi)^3} M_{p_1 p_2 \rightarrow k l'} [M_{p'_1 p'_2 \rightarrow k l'}]^* \\ & \left(\frac{1}{E_{p_1} + E_{p_2} - E_k - E_{l'}} \right)^* \left(\frac{1}{E_k + E_{l'} - E_{p'_1} - E_{p'_2}} \right)^* \left(\frac{1}{2E_k} \right)^* \left(\frac{1}{2E_{l'}} \right)^* \\ &= -\left(\frac{1}{R}\right)^2 \frac{1}{C_\phi} \frac{1}{8E_{p_1} E_\gamma} |M_{\gamma^* p_1 \rightarrow k'}|^2 (2\pi)^4 \delta^4(p_\gamma + p_1 - k') \frac{d^3 k'}{(2\pi)^3 2E_{k'}} \\ & \frac{E_k}{\sqrt{E_{p_1} + E_{p_2}} \sqrt{E_{p'_1} + E_{p'_2}}} M_{p_1 p_2 \rightarrow k l'} [M_{p'_1 p'_2 \rightarrow k l'}]^* \left(\frac{1}{E_{p_1} + E_{p_2} - E_k - E_{l'}} \right)^2 \\ & \left(\frac{1}{2E_k} \right)^2 \frac{d^3 l'}{(2\pi)^3 2E_{l'}}, \end{aligned} \quad (5.10)$$

where the factor of $\frac{1}{2}$ in (5.7) is needed for the cancellation of IR-divergences and momentum conservation as we shall discuss shortly. One can re-understand this factor as follows: only half of the probe-vertex connects with the partonic matrix in figs. 5c-f as well as in figs. 4b-c, and the square root of the parton density accepts the contributions of the partonic processes through a parton line. That is,

$$\frac{\sqrt{q} d\sqrt{q}}{d \ln Q^2} = \frac{1}{2} \frac{dq}{d \ln Q^2}. \quad (5.11)$$

Since, for the given initial partons we have,

$$\sum_{s,t,u} M_{p_1 p_2 \rightarrow kl'} [M_{p'_1 p'_2 \rightarrow kl'}]^* > 0, \quad (5.12)$$

we can conclude that the negative sign in eq. (5.10) arises from

$$\frac{1}{E_{p_1} + E_{p_2} - E_k - E_{l'}} \frac{1}{E_k + E_{l'} - E_{p'_1} - E_{p'_2}} = - \left(\frac{1}{E_{p_1} + E_{p_2} - E_k - E_{l'}} \right)^2. \quad (5.13)$$

In consequence, we have

$$\begin{aligned} \frac{d\phi(x_B, Q^2)}{d \ln Q^2} &= -\frac{1}{2} \left(\frac{1}{RQ} \right)^2 \int f(x_1, x_2; x'_1, x'_2, Q^2) \delta(x_1 + x_2 - x'_1 - x'_2) \\ &\quad P_4^{(2-2)}(x_1, x_2, x'_1, x'_2, x_3, x_4) \\ &\quad \delta(x_1 - x_B) \delta(x_1 + x_2 - x_3 - x_4) dx_1 dx_2 dx'_1 dx'_2 dx_3 dx_4. \end{aligned} \quad (5.14)$$

Comparing eqs. (5.14) with (5.6), we see that the same recombination function appears in both cases. We can calculate the contributions of figs. 5a–f in TOPT using the same method, and finally obtain the hard contribution as

$$\begin{aligned} \frac{d\phi(x_B, Q^2)}{d \ln Q^2} &= \left(\frac{1}{RQ} \right)^2 \int f(x_1, x_2; x'_1, x'_2, Q^2) P_4^{(2-2)}(x_1, x_2, x'_1, x'_2, x_3, x_4) \\ &\quad \delta(x_1 + x_2 - x'_1 - x'_2) [\delta(x_3 - x_B) + \delta(x_4 - x_B) - \frac{1}{2} \delta(x_1 - x_B) \\ &\quad - \frac{1}{2} \delta(x'_1 - x_B) - \frac{1}{2} \delta(x_2 - x_B) - \frac{1}{2} \delta(x'_2 - x_B)] \\ &\quad \delta\left(\frac{1}{2}x_1 + \frac{1}{2}x'_1 + \frac{1}{2}x_2 + \frac{1}{2}x'_2 - x_3 - x_4\right) dx_1 dx_2 dx'_1 dx'_2 dx_3 dx_4. \end{aligned} \quad (5.15)$$

Obviously, eq. (5.14) contains the momentum conservation condition:

$$\frac{d \int_0^1 x_B \phi(x_B, Q^2) dx_B}{d \ln Q^2} = 0. \quad (5.16)$$

This completes the discussion of the first type of diagrams. As the next step, we discuss the interference terms, $M_{p\gamma^* \rightarrow k'l'X}^{(2-1)} [M_{p\gamma^* \rightarrow k'l'X}^{(2-3)}]^*$, shown in fig. 7. Proceeding similarly, we obtain the contributions from the interference processes in fig. 7 to be

$$\begin{aligned} \frac{d\phi(x_B, Q^2)}{d \ln Q^2} &= 2P_{inter} \left(\frac{1}{RQ} \right)^2 \int f(x_1; x_2, x'_1, x'_2, Q^2) P_4^{(1-3)}(x_1, x_2, x'_1, x'_2, x_3, x_4) \\ &\quad \delta(x_1 - x_2 - x'_1 - x'_2) [\delta(x_3 - x_B) + \delta(x_4 - x_B) - \frac{1}{2} \delta(x_1 - x_B) \\ &\quad - \frac{1}{2} \delta(x'_1 - x_B) - \frac{1}{2} \delta(x_2 - x_B) - \frac{1}{2} \delta(x'_2 - x_B)] \end{aligned}$$

$$\delta(x_1 - x_3 - x_4)dx_1dx_2dx'_1dx'_2dx_3dx_4, \quad (5.17)$$

where

$$\begin{aligned} f(x_1; x_2, x'_1, x'_2, Q^2) &= \frac{\sqrt{E_{p_1} + E_{p_2}}\sqrt{E_{p'_1} + E_{p'_2}}}{E_p} M_{p \rightarrow p_1 X} [M_{p \rightarrow p'_1 p'_2 p_2 X}]^* \\ &\frac{1}{E_p - E_{p_1} - E_{X'}} \left(\frac{1}{E_p - E_{p'_1} - E_{p'_2} - E_{p_2} - E_X} \right)^* \frac{1}{2E_{p_1}} \frac{1}{2E_{p_2}} \frac{1}{2E_{p'_1}} \frac{1}{2E_{p'_2}} \prod_X \frac{d^3 k_X}{(2\pi)^3 2E_X} \\ &H(\gamma^* p_1 p_2 \rightarrow \gamma^* p'_1 p'_2). \end{aligned} \quad (5.18)$$

and

$$\begin{aligned} &P_4^{(1-3)}(x_1, x_2, x'_1, x'_2, x_3, x_4) dx_4 \frac{dl_\perp^2}{l_\perp^4} \\ &= \frac{E_k}{\sqrt{E_{p_1} + E_{p_2}}\sqrt{E_{p'_1} + E_{p'_2}}} M_{p_1 \rightarrow kl'} [M_{p'_1 p'_2 p_2 \rightarrow kl'}]^* \\ &\frac{1}{E_k + E'_l - E_{p_1}} \frac{1}{E_k + E_{l'} - E_{p'_1} - E_{p'_2} - E_{p_2}} \left(\frac{1}{2E_k} \right)^2 \frac{d^3 l'}{(2\pi)^3 2E_{l'}}. \end{aligned} \quad (5.19)$$

In eq. (5.17), $P_{inter} = 0$ or 1 implies that the interference processes are inhibited or exhibited, respectively. Now an interesting observation is that $P_4^{(2-2)}$ and $P_4^{(1-3)}$ are really similar except for a simple coefficient and the different variable range. In fact, from fig. 8 we find

$$P_4^{(2-2)} = -\xi P_4^{(1-3)}, \quad (5.20)$$

where ξ is defined below and the negative sign occurs because $(l_\perp^2/(2x_l p) - l_\perp^2/(2x_{l'} p))$ changes its sign from $x_l < x_{l'}$ to $x_l > x_{l'}$ in fig. 8. The contributions of the vertices A and B have same form, since the momenta of the partons a and b are $[x_a p, 0, x_a p]$ and $[x_b p, 0, x_b p]$, respectively. The factor ξ arises from the following symmetry: if both the final partons are gluons or quarks (we do not distinguish quarks and antiquarks in this work), the corresponding virtual diagrams in figs. 7c-f are symmetric under the exchange of these two partons. However, this symmetry will be lost if we use $P_4^{(2-2)}$ to replace $P_4^{(1-3)}$. In this case, $\xi = 1/2$, otherwise, $\xi = 1$.

It seems that there are different energy deficits in going from $P_4^{(1-3)}$ to $P_4^{(2-2)}$ in the ATOPT: $1/(E_k + E_{l'} - E_{p_1})$ in $P_4^{(1-3)}$ and $1/(E_k + E_{l'} - E_{p_1} - E_{p_2})$ in $P_4^{(2-2)}$; $1/(E_k + E_{l'} - E_{p'_1} - E_{p'_2} - E_{p_2})$ in $P_4^{(1-3)}$ and $1/(E_k + E_{l'} - E_{p'_1} - E_{p'_2})$ in $P_4^{(2-2)}$. However, they are really the same factor, arising from the term, $(l_\perp^2/(2x_3 p) + l_\perp^2/(2x_4 p))^{-1}$.

Therefore, one can replace $P_4^{(1-3)}$ by $P_4^{(2-2)}$ and reconstruct eq. (5.17), where the terms $f(x_1; x'_1, x'_2, x_2, Q^2)$ and $\delta(x_1 - x'_1 - x'_2 - x_2)$ should be replaced by $f(x_1, x_2; x'_1, x'_2, Q^2)$ and $\delta(x_1 + x_2 - x'_1 - x'_2)$, respectively, since x_i are the scaling variables.

The final results from fig. 7 are

$$\frac{d\phi(x_B, Q^2)}{d \ln Q^2}$$

$$\begin{aligned}
&= 2\left(\frac{1}{RQ}\right)^2 P_{inter} \int f(x_1, x_2; x'_1, x'_2, Q^2) P_4^{(2-2)}(x_1, x_2, x'_1, x'_2, x_3, x_4) \\
&\quad \delta(x_1 + x_2 - x'_1 - x'_2) [-\delta(x_3 - x_B) - \delta(x_4 - x_B) + \frac{1}{2}\delta(x_1 - x_B) \\
&\quad + \frac{1}{2}\delta(x'_1 - x_B) + \frac{1}{2}\delta(x_2 - x_B) + \frac{1}{2}\delta(x'_2 - x_B)] \\
&\quad \delta\left(\frac{1}{2}x_1 + \frac{1}{2}x'_1 + \frac{1}{2}x_2 + \frac{1}{2}x'_2 - x_3 - x_4\right) dx_1 dx_2 dx'_1 dx'_2 dx_3 dx_4. \tag{5.21}
\end{aligned}$$

Obviously, the momentum conservation condition is also satisfied in eq. (5.21),

$$\frac{d \int_0^1 x_B \phi(x_B, Q^2) dx_B}{d \ln Q^2} = 0. \tag{5.22}$$

6 Parton correlation functions

In general, the parton density is a concept that is only defined at the twist-2 level; it can be expressed in terms of the product of the initial and final hadronic wave functions with the same parton configuration. The parton correlation function $f(x_1, x_2; x'_1, x'_2)$ is a generalization of the parton density beyond the leading twist. It has not yet been experimentally observed. In this section, therefore, we shall try to construct the connection between the parton correlation function and the parton density.

For example, consider the correlation function for the case when $x_1 = x'_1$ and $x_2 = x'_2$ in eq.(5.8); this is given by

$$\begin{aligned}
&f(x_1, x_2; x_1, x_2) \\
&= \frac{E_{p_1} E_{p_2}}{E_p} |M_{p \rightarrow p_1 p_2 X}|^2 \left(\frac{1}{E_{p_1} + E_{p_2} + E_X - E_p}\right)^2 \left(\frac{1}{2E_{p_1}}\right)^2 \left(\frac{1}{2E_{p_2}}\right)^2 \prod_X \frac{d^3 k_X}{(2\pi)^3 2E_X} \\
&= \rho(x_1, x_2), \tag{6.1}
\end{aligned}$$

and is the number density of two partons, i.e., the probability of simultaneously finding two partons carrying x_1 and x_2 fractions of the proton momentum respectively. In the quantum mechanics approximation, we can use wave functions to represent $\rho(x_1, x_2)$ as

$$\rho(x_1, x_2) = \psi(x_1, x_2) \psi^*(x_1, x_2), \tag{6.2}$$

where $\psi(x_1, x_2)$ is the wave function of two partons in the proton. Similarly, we express the parton correlation function as the product of the initial and final hadron wave functions with different parton momentum, that is

$$f(x_1, x_2; x'_1, x'_2) = \psi(x_1, x_2) \psi^*(x'_1, x'_2). \tag{6.3}$$

We define

$$\bar{f}(x_1, x_2; x'_1, x'_2) \equiv \psi(x'_1, x'_2) \psi^*(x_1, x_2) = \kappa^2 f(x_1, x_2; x'_1, x'_2). \tag{6.4}$$

Therefore, we have

$$\begin{aligned}
f(x_1, x_2; x'_1, x'_2) &= \kappa^{-1} \sqrt{f(x_1, x_2; x'_1, x'_2) \bar{f}(x_1, x_2; x'_1, x'_2)} \\
&= \kappa^{-1} \sqrt{\psi(x_1, x_2) \psi^*(x_1, x_2) \psi(x'_1, x'_2) \psi^*(x'_1, x'_2)} \\
&= \kappa^{-1} \sqrt{\rho(x_1, x_2) \rho(x'_1, x'_2)}.
\end{aligned} \tag{6.5}$$

In general, the two-parton number density can be approximated by

$$\rho(x_1, x_2) = q_a(x_1) q_b(x_2) R_{ab}^2(x_1, x_2), \tag{6.6}$$

where $R_{ab}^2(x_1, x_2)$ is the momentum correlation of two initial partons; $q_a(x_1)$ and $q_b(x_2)$ are the parton number densities.

In order to estimate the value of κ in eq. (6.5), we consider the process shown in fig. 9. The time reversal invariance requires that

$$d\sigma(\gamma^* p \rightarrow \gamma^* p) = d\sigma(\gamma^* p \leftarrow \gamma^* p), \tag{6.7}$$

or

$$\psi(x_1, x_2) AB^* \psi^*(x'_1, x'_2) = \psi(x'_1, x'_2) BA^* \psi^*(x_1, x_2), \tag{6.8}$$

where A and B are the contributions of the hard parts in fig. 9. Therefore,

$$\begin{aligned}
\kappa &= \sqrt{\frac{\bar{f}(x_1, x_2; x'_1, x'_2)}{f(x_1, x_2; x'_1, x'_2)}} \\
&= \sqrt{\frac{AB^*}{BA^*}}.
\end{aligned} \tag{6.9}$$

Since κ is expressible in terms of hard parts, eq. (6.9) indicates that κ is calculable within PQCD.

7 New evolution equations

We now apply the method, used to describe scalar partons in Section 5, to the realistic case of partons (quarks and gluons) interacting within QCD. In consequence, we have following new evolution equations with twist-4 for $GG \rightarrow q\bar{q}$ and $GG \rightarrow GG$ respectively:

(a) $GG \rightarrow q\bar{q}$. The contribution to the evolution equation for gluons is,

$$\begin{aligned}
&\frac{dG(x_B, Q^2)}{d \ln Q^2} \\
&= \left(\frac{1}{RQ}\right)^2 \int \sqrt{G(x_1, Q^2) G(x_2, Q^2) G(x_1 + \Delta, Q^2) G(x_2 - \Delta, Q^2)} \\
&\quad R_{GG}(x_1, x_2) R_{GG}(x_1 + \Delta, x_2 - \Delta) \\
&\quad \sum_i \kappa_i^{-1} P_{GG \rightarrow q\bar{q}}^i(x_1, x_2, x_3, x_4, \Delta) \delta(x_1 + x_2 - x_3 - x_4)
\end{aligned}$$

$$\begin{aligned}
& [-\frac{1}{2}\delta(x_1 - x_B) - \frac{1}{2}\delta(x_1 + \Delta - x_B) - \frac{1}{2}\delta(x_2 - x_B) - \frac{1}{2}\delta(x_2 - \Delta - x_B)]dx_1dx_2dx_3dx_4d\Delta \\
& + 2(\frac{1}{RQ})^2 P_{inter.} \int \sqrt{G(x_1, Q^2)G(x_2, Q^2)G(x_1 + \Delta, Q^2)G(x_2 - \Delta, Q^2)} \\
& R_{GG}(x_1, x_2)R_{GG}(x_1 + \Delta, x_2 - \Delta) \\
& \sum_i \kappa_i^{-1} P_{GG \rightarrow q\bar{q}}^i(x_1, x_2, x_3, x_4, \Delta) \delta(x_1 + x_2 - x_3 - x_4) \\
& \frac{1}{2} [\frac{1}{2}\delta(x_1 - x_B) + \frac{1}{2}\delta(x_1 + \Delta - x_B) + \frac{1}{2}\delta(x_2 - x_B) + \frac{1}{2}\delta(x_2 - \Delta - x_B)]dx_1dx_2dx_3dx_4d\Delta, \quad (7.1)
\end{aligned}$$

where the factor $\frac{1}{2}$ in the last factor arises from symmetry considerations, just as in eq. (5.20). However, this symmetry will be broken due to the cut in real diagrams in the corresponding equation for quarks:

$$\begin{aligned}
& \frac{dq(x_B, Q^2)}{d \ln Q^2} \\
& = (\frac{1}{RQ})^2 \int \sqrt{G(x_1, Q^2)G(x_2, Q^2)G(x_1 + \Delta, Q^2)G(x_2 - \Delta, Q^2)} \\
& R_{GG}(x_1, x_2)R_{GG}(x_1 + \Delta, x_2 - \Delta) \\
& \sum_i \kappa_i^{-1} P_{GG \rightarrow q\bar{q}}^i(x_1, x_2, x_3, x_4, \Delta) \delta(x_1 + x_2 - x_3 - x_4) [\delta(x_3 - x_B) + \delta(x_4 - x_B)] dx_1 dx_2 dx_3 dx_4 d\Delta \\
& + 2(\frac{1}{RQ})^2 P_{inter} \int \sqrt{G(x_1, Q^2)G(x_2, Q^2)G(x_1 + \Delta, Q^2)G(x_2 - \Delta, Q^2)} \\
& R_{GG}(x_1, x_2)R_{GG}(x_1 + \Delta, x_2 - \Delta) \\
& \sum_i \kappa_i^{-1} P_{GG \rightarrow q\bar{q}}^i(x_1, x_2, x_3, x_4, \Delta) \delta(x_1 + x_2 - x_3 - x_4) \\
& [-\delta(x_3 - x_B) - \delta(x_4 - x_B)] dx_1 dx_2 dx_3 dx_4 d\Delta. \quad (7.2)
\end{aligned}$$

(b) $GG \rightarrow GG$. The contribution to the evolution equation for gluons is,

$$\begin{aligned}
& \frac{dG(x_B, Q^2)}{d \ln Q^2} \\
& = (\frac{1}{RQ})^2 \int \sqrt{G(x_1, Q^2)G(x_2, Q^2)G(x_1 + \Delta, Q^2)G(x_2 - \Delta, Q^2)} \\
& R_{GG}(x_1, x_2)R_{GG}(x_1 + \Delta, x_2 - \Delta) \\
& \sum_i \kappa_i^{-1} P_{GG \rightarrow GG}^i(x_1, x_2, x_3, x_4, \Delta) \delta(x_1 + x_2 - x_3 - x_4) \\
& [\delta(x_3 - x_B) + \delta(x_4 - x_B) - \frac{1}{2}\delta(x_1 - x_B) - \frac{1}{2}\delta(x_1 + \Delta - x_B) - \frac{1}{2}\delta(x_2 - x_B) - \frac{1}{2}\delta(x_2 - \Delta - x_B)] \\
& dx_1 dx_2 dx_3 dx_4 d\Delta \\
& + 2(\frac{1}{RQ})^2 P_{inter} \int \sqrt{G(x_1, Q^2)G(x_2, Q^2)G(x_1 + \Delta, Q^2)G(x_2 - \Delta, Q^2)}
\end{aligned}$$

$$\begin{aligned}
& R_{GG}(x_1, x_2) R_{GG}(x_1 + \Delta, x_2 - \Delta) \\
& \sum_i \kappa_i^{-1} P_{GG \rightarrow GG}^i(x_1, x_2, x_3, x_4, \Delta) \delta(x_1 + x_2 - x_3 - x_4) \\
& [-\delta(x_3 - x_B) - \delta(x_4 - x_B) + \frac{1}{4}\delta(x_1 - x_B) + \frac{1}{4}\delta(x_1 + \Delta + x_B) + \frac{1}{4}\delta(x_2 - x_B) + \frac{1}{4}\delta(x_2 - \Delta - x_B)] \\
& dx_1 dx_2 dx_3 dx_4 d\Delta.
\end{aligned} \tag{7.3}$$

We discuss the case when $P_{inter} = 1$ and 0 separately.

A: $P_{inter} = 1$. We can take $P_{inter} = 1$ if there is no reason to forbid three-parton recombination in the interference terms in nucleon. Thus, we have

$$\begin{aligned}
& \frac{dG(x_B, Q^2)}{d \ln Q^2} \\
& = \left(\frac{1}{RQ}\right)^2 \int_{(x_1+x_2) \geq x_B} \sqrt{G(x_1, Q^2) G(x_2, Q^2) G(x_1 + \Delta, Q^2) G(x_2 - \Delta, Q^2)} \\
& \quad R_{GG}(x_1, x_2) R_{GG}(x_1 + \Delta, x_2 - \Delta) \\
& \quad \sum_i \kappa_i^{-1} P_{GG \rightarrow GG}^i(x_1, x_2, x_3, x_4, \Delta) \delta(x_1 + x_2 - x_3 - x_4) \\
& \quad [\delta(x_3 - x_B) + \delta(x_4 - x_B)] dx_1 dx_2 dx_3 dx_4 d\Delta \\
& - 2 \left(\frac{1}{RQ}\right)^2 \int_{x_1 \geq x_B} \sqrt{G(x_1, Q^2) G(x_2, Q^2) G(x_1 + \Delta, Q^2) G(x_2 - \Delta, Q^2)} \\
& \quad R_{GG}(x_1, x_2) R_{GG}(x_1 + \Delta, x_2 - \Delta) \\
& \quad \sum_i \kappa_i^{-1} P_{GG \rightarrow GG}^i(x_1, x_2, x_3, x_4, \Delta) \delta(x_1 + x_2 - x_3 - x_4) \\
& \quad [\delta(x_3 - x_B) + \delta(x_4 - x_B)] dx_1 dx_2 dx_3 dx_4 d\Delta.
\end{aligned} \tag{7.4}$$

and

$$\begin{aligned}
& \frac{dq(x_B, Q^2)}{d \ln Q^2} \\
& = \left(\frac{1}{RQ}\right)^2 \int_{(x_1+x_2) \geq x_B} \sqrt{G(x_1, Q^2) G(x_2, Q^2) G(x_1 + \Delta, Q^2) G(x_2 - \Delta, Q^2)} \\
& \quad R_{GG}(x_1, x_2) R_{GG}(x_1 + \Delta, x_2 - \Delta) \\
& \quad \sum_i \kappa_i^{-1} P_{GG \rightarrow q\bar{q}}^i(x_1, x_2, x_3, x_4, \Delta) \delta(x_1 + x_2 - x_3 - x_4) \\
& \quad [\delta(x_3 - x_B) + \delta(x_4 - x_B)] dx_1 dx_2 dx_3 dx_4 d\Delta \\
& - 2 \left(\frac{1}{RQ}\right)^2 \int_{x_1 \geq x_B} \sqrt{G(x_1, Q^2) G(x_2, Q^2) G(x_1 + \Delta, Q^2) G(x_2 - \Delta, Q^2)} \\
& \quad R_{GG}(x_1, x_2) R_{GG}(x_1 + \Delta, x_2 - \Delta) \\
& \quad \sum_i \kappa_i^{-1} P_{GG \rightarrow q\bar{q}}^i(x_1, x_2, x_3, x_4, \Delta) \delta(x_1 + x_2 - x_3 - x_4)
\end{aligned}$$

$$[\delta(x_3 - x_B) + \delta(x_4 - x_B)]dx_1dx_2dx_3dx_4d\Delta. \quad (7.5)$$

Equations (7.4) and (7.5) predict that the shadowing effect in quark distributions is stronger than that in the gluon distribution, since there are two shadowing sources for quarks but only one shadowing source for gluons.

B: $P_{inter} = 0$. This means that the interference terms are forbidden. An example of such a case is the radiation recombination in a nucleus. We consider the recombination of partons which originate from different nucleons in a nucleus. A single parton can not escape from the confinement region of a nucleon, unless it forms a colour-single cluster with other partons. We define the probability of a parton leaks out from the confined volume as w . Thus,

$$M^{(2-2)}(x_1, x_2 \rightarrow x_3, x_4)[M^{(2-2)}(x_1, x_2 \rightarrow x_3, x_4)]^* \propto w, \quad (7.6)$$

and

$$\begin{aligned} & M^{(2-1)}(x_1 \rightarrow x_3, x_4)[M^{(2-3)}(x_2, x'_1, x'_2 \rightarrow x_3, x_4)]^* \\ & + M^{(2-3)}(x_2, x'_1, x'_2 \rightarrow x_3, x_4)[M^{(2-1)}(x_1 \rightarrow x_3, x_4)]^* \propto w^3, \end{aligned} \quad (7.7)$$

We can neglect the interference processes (7.7), because of the confinement condition $w < 1$. In this case, we have another face of the evolution equation:

$$\begin{aligned} & \frac{dG(x_B, Q^2)}{d \ln Q^2} \\ & = \left(\frac{1}{RQ}\right)^2 \int \sqrt{G(x_1, Q^2)G(x_2, Q^2)G(x_1 + \Delta, Q^2)G(x_2 - \Delta, Q^2)} \\ & \quad R_{GG}(x_1, x_2)R_{GG}(x_1 + \Delta, x_2 - \Delta) \\ & \quad \sum_i \kappa_i^{-1} P_{GG \rightarrow GG}^i(x_1, x_2, x_3, x_4, \Delta) \delta(x_1 + x_2 - x_3 - x_4) \\ & [\delta(x_3 - x_B) + \delta(x_4 - x_B) - \frac{1}{2}\delta(x_1 - x_B) - \frac{1}{2}\delta(x_1 + \Delta - x_B) - \frac{1}{2}\delta(x_2 - x_B) - \frac{1}{2}\delta(x_2 - \Delta - x_B)] \\ & \quad dx_1dx_2dx_3dx_4d\Delta \\ & - \left(\frac{1}{RQ}\right)^2 \int \sqrt{G(x_1, Q^2)G(x_2, Q^2)G(x_1 + \Delta, Q^2)G(x_2 - \Delta, Q^2)} \\ & \quad R_{GG}(x_1, x_2)R_{GG}(x_1 + \Delta, x_2 - \Delta) \\ & \quad \sum_i \kappa_i^{-1} P_{GG \rightarrow q\bar{q}}^i(x_1, x_2, x_3, x_4, \Delta) \delta(x_1 + x_2 - x_3 - x_4) \\ & \quad \left[\frac{1}{2}\delta(x_1 - x_B) + \frac{1}{2}\delta(x_1 + \Delta - x_B) + \frac{1}{2}\delta(x_2 - x_B) + \frac{1}{2}\delta(x_2 - \Delta - x_B)\right] \\ & \quad dx_1dx_2dx_3dx_4d\Delta. \end{aligned} \quad (7.8)$$

and

$$\begin{aligned}
& \frac{dq(x_B, Q^2)}{d \ln Q^2} \\
&= \left(\frac{1}{RQ}\right)^2 \int \sqrt{G(x_1, Q^2)G(x_2, Q^2)G(x_1 + \Delta, Q^2)G(x_2 - \Delta, Q^2)} \\
& \quad R_{GG}(x_1, x_2)R_{GG}(x_1 + \Delta, x_2 - \Delta) \\
& \sum_i \kappa_i^{-1} P_{GG \rightarrow q\bar{q}}^i(x_1, x_2, x_3, x_4, \Delta) \delta(x_1 + x_2 - x_3 - x_4) [\delta(x_3 - x_B) + \delta(x_4 - x_B)] dx_1 dx_2 dx_3 dx_4 d\Delta
\end{aligned} \tag{7.9}$$

Now the sign of the right-hand side of eq. (7.9) is positive. This means that the shadowing in quark distribution is weaker than that in gluon distribution.

In principle, we can calculate the parton recombination functions at order $\mathcal{O}(\alpha_s^2)$ for every parton flavors in the whole x region. However, in the majority of cases, the parton recombination is happened in the gluons with small x . For simplicity, we only consider the case where all partons are gluons with small x value in this work. We will discuss the recombination of partons in a general x range elsewhere. In this approximation, we can use the results of Mueller and Qiu in the calculations of the real process of fig. 1a in ref. [2]. Thus, the contributions of figs. 6a,b to $P_4^{(2-2)}$ are from t- and u-channels and as well as their interference-terms. One obtains

$$\sum_i \kappa_i^{-1} P_i^{(GG-GG)} \simeq \frac{\pi^3}{N^2 - 1} \left(\frac{\alpha_s C_A}{\pi}\right)^2 \frac{x_4}{x_1^2}, \tag{7.10}$$

where we assume that $x_1 = x'_1 = x_2 = x'_2$. Eq. (7.10) evaluates to

$$\begin{aligned}
& 2 \int \sum_i \kappa_i^{-1} P_i^{(GG-GG)} \delta(x_3 - x_B) \delta(2x_1 - x_3 - x_4) dx_1 dx_3 dx_4 \\
&= \frac{4\pi^3}{N^2 - 1} \left(\frac{\alpha_s C_A}{\pi}\right)^2 \int \frac{dx_1}{x_1},
\end{aligned} \tag{7.11}$$

which is the same as the result of ref. [2]. If we take the gluon correlation function [2] to be

$$\frac{1}{R^2} G^{(2)}(x_1, x'_1, x_2, x'_2, Q^2) = \frac{9}{8\pi R^2} G(x_1, Q^2) G(x_1, Q^2), \tag{7.12}$$

we obtain the following simplified evolution equations arising from $GG \rightarrow GG$ in the small x region:

$$\begin{aligned}
& \frac{dx_B G(x_B, Q^2)}{d \ln Q^2} = -\frac{81}{16} \left(\frac{\alpha_s}{RQ}\right)^2 \frac{[x_B G(x_B, Q^2)]^2}{x_B} \\
& + \frac{81}{16} \left(\frac{\alpha_s}{RQ}\right)^2 x_B \int_{x_B/2}^{1/2} \frac{[x_1 G(x_1, Q^2)]^2}{x_1^3} dx_1 \\
& + P_{inter} \frac{81}{16} \left(\frac{\alpha_s}{RQ}\right)^2 \frac{[x_B G(x_B, Q^2)]^2}{x_B}
\end{aligned}$$

$$-P_{inter} \frac{81}{8} \left(\frac{\alpha_s}{RQ}\right)^2 x_B \int_{x_B}^{1/2} \frac{[x_1 G(x_1, Q^2)]^2}{x_1^3} dx_1. \quad (7.13)$$

Note that the modifications of fig. 5a-b are related to $G(x_B, Q^2)$ in eq. (7.13) but not to $x_B G(x_B, Q^2)$ according to eq. (5.1) in our work. However, these real diagrams fig. 5a-b (or fig. 1a) in ref. [2] are regarded as the modifications in $x_B G(x_B, Q^2)$. Therefore, the equation (7.13) is different with the GLR equation in the dependencies of x_1 and x_B .

In consequence, the new evolution equations if $P_{inter} = 1$ are

$$\begin{aligned} \frac{dx_B G(x_B, Q^2)}{d \ln Q^2} &= \frac{81}{16} \left(\frac{\alpha_s}{RQ}\right)^2 x_B \int_{x_B/2}^{1/2} \frac{[x_1 G(x_1, Q^2)]^2}{x_1^3} dx_1 \\ &\quad - \frac{81}{8} \left(\frac{\alpha_s}{RQ}\right)^2 x_B \int_{x_B}^{1/2} \frac{[x_1 G(x_1, Q^2)]^2}{x_1^3} dx_1. \end{aligned} \quad (7.14)$$

Here, we have an extra conservation

$$\frac{\int_0^1 dx_B x_B G(x_B, Q^2)}{d \ln Q^2} \equiv 0, \quad (7.15)$$

since for any function $f(x_1)$ we have

$$\int_0^1 dx_B \int_{x_B/2}^{1/2} f(x_1) dx_1 - 2 \int_0^{1/2} dx_B \int_{x_B}^{1/2} f(x_1) dx_1 \equiv 0. \quad (7.16)$$

On the other hand, the new equation has following different form if $P_{inter} = 0$

$$\begin{aligned} &\frac{dx_B G(x_B, Q^2)}{d \ln Q^2} \\ &= -\frac{81}{16} \left(\frac{\alpha_s}{RQ}\right)^2 \frac{[x_B G(x_B, Q^2)]^2}{x_B} + \frac{81}{16} \left(\frac{\alpha_s}{RQ}\right)^2 x_B \int_{x_B/2}^{1/2} \frac{[x_1 G(x_1, Q^2)]^2}{x_1^3} dx_1. \end{aligned} \quad (7.17)$$

8 Discussions and conclusions

The following interesting components of the new evolution equation derived in this paper are highlighted:

1. Through the derivations of sections 4 and 5, it seems there is an interesting “cutting rule” in DIS: The contributions of the cut diagrams in the sum (3.4) have the identical integral kernel with only the following different factors R :

$$R = (\pm) \times (1, \frac{1}{2}) \times \delta(x_\beta - x_B). \quad (8.1)$$

The various terms appearing in the cutting rule (8.1) can be described in terms of the general structure of the cut diagrams $G_\gamma(N)$ in TOPT:

$$G_\gamma(N) = \prod_{\text{left-vertices}} \frac{1}{\sum_{a' \in i+1} E_{a'} - \sum_{a \in i} E_a} \prod_{\text{right-vertices}} \frac{1}{\sum_{b \in j} E_b - \sum_{b' \in j+1} E_{b'}}$$

$$\prod_{\text{vertices}-k} \delta(\sum_f x_f = 0) \prod_{\text{states}-c} \frac{1}{2E_c} \prod_{\text{loops}-d} \frac{d^3 \mathbf{k}_d}{(2\pi)^3} \prod_{\text{final}-\text{states}-e} \frac{d^3 \mathbf{k}_e}{(2\pi^3)^3 2E_e} N_G, \quad (8.2)$$

where N_G is an overall numerator-and-symmetry factor and is independent of the cut γ [6]; i and $i+1$ (or j and $j+1$) are the time-ordered lines on the left- (or right-) vertices; $\delta(\sum_f x_f = 0)$ is the conservation of longitudinal momentum at the vertex.

- (a) The sign in the first factor of (8.1) is determined by the energy deficits in (8.2). For example, if a vertex pass through the cut line, the corresponding energy deficit will change its sign since

$$\frac{1}{\sum_{a' \in i+1} E_{a'} - \sum_{a \in i} E_a} \rightarrow \frac{1}{\sum_{a \in i} E_a - \sum_{a' \in i+1} E_{a'}}, \quad (8.3)$$

as we have for example in (4.11).

- (b) The second factor takes a value of 1/2 if the probe-vertex inserts in the initial line as shown in (5.11).
(c) $\delta(x_\beta - x_B)$ is the direct result of the sum (3.4).
(d) When the cut line moves its position, the contributions of the final states in (8.2) will change the momentum-symbols, but don't change the structure of the intermediate state according to the sum-condition I in (3.4). We also note that a virtual parton line has 4-dimensional integral and a real parton only a 3-dimensional integral in the covariant perturbation theory; however, in TOPT, since the virtual partons are replaced by the effective real partons, the above mentioned differences are contained in the energy deficits. In particular, when the cut line moves to cutting line c from cutting a loop $d-d'$ in the process of $c \rightarrow d'd \rightarrow e$, we have similar expressions in (8.2) due to

$$\frac{1}{2E_c} \frac{d^3 \mathbf{k}_{d'}}{(2\pi)^3 2E_{d'}} \frac{d^3 \mathbf{k}_d}{(2\pi)^3 2E_d} \rightarrow \frac{d^3 \mathbf{k}_c}{(2\pi)^3 2E_c} \frac{d^3 \mathbf{k}_d}{(2\pi)^3} \frac{1}{2E_d} \frac{1}{2E_{d'}}. \quad (8.4)$$

Thus, as the cut line moves from cutting a loop to uncutting a loop, the integral kernel has the same form. The difference lies only in the cutting positions.

- (e) The cut line can also cut the nonperturbative matrix elements with multi-initial partons. The reason is that the initial parton line on the light-cone can be moved from one-side of the cut to another side (see fig.6) [13, 14]. Thus, we can use the same correlation function to represent the different hadronic parts and keep the same integral kernel. Because of this important property, the sum (3.4) shall include more complex cut diagrams when we study parton fusion or recombination.
(f) Finally, the matrix can be factorized to obtain the probability explanation; the reason is that we used the bare probe-vertex approximation and the coefficient C_q in (2.2) (or C_ϕ in (5.2)) is canceled in the calculations at this approximation.

2. In the DGLAP equation, there are IR-divergences when a final-state gluon becomes soft. These IR-divergences can be taken care of by the sum of figs. 4 according to eqs. (3.4) and (8.1). The divergences in (7.11) are canceled due to the symmetry at small x approximation [2]. However, a soft initial parton also may give rise to IR-divergences in the parton recombination process in a general case. We now show that such IR-divergences can be canceled by using the same method in the DGLAP equation.

For example, take $x_2 = 0$ in fig. 10; this implies $p_2 = 0$. Since the unpolarized structure functions only involve contributions from terms with even-twist, we have $x'_2 = 0$ at $x_2 = 0$. The momentum of l_L and l_R are determined by the down-vertices since the energy is not conserved in the up-vertices in the TOPT, i.e., $l_L = [(x_2 - x_4)P - \frac{l_1^2}{2x_4P}, l_\perp, (x_2 - x_4)P]$ and $l_R = [(x_4 - x'_2)P + \frac{l_1^2}{2x_4P}, -l_\perp, (x_4 - x'_2)P]$. Thus, $x_4 = 0$ and $x_1 = x'_1 = x_3$. According to (5.14), we can find that

$$\begin{aligned} & \int f(x_1 = x_B, x_2 = 0, x'_1 = x_B, x'_2 = 0, Q^2) \\ & [P_4^{(2-2)}(x_1 = x_3, x_2 = 0, x'_1 = x_3, x'_2 = 0, x_3, x_4 = 0)\delta(x_3 - x_B)dx_3 \\ & - \frac{1}{2}P_4^{(2-2)}(x_1, x_2 = 0, x'_1 = x_1, x'_2 = 0, x_3 = x_1, x_4 = 0)\delta(x_1 - x_B)dx_1 \\ & - \frac{1}{2}P_4^{(2-2)}(x_1 = x'_1, x_2 = 0, x'_1, x'_2 = 0, x_3 = x'_1, x_4 = 0)\delta(x'_1 - x_B)dx'_1] = 0. \end{aligned} \quad (8.5)$$

Therefore, IR-divergences can be canceled point-by-point at the IR-pole.

3. Obviously, the new evolution equations (7.4), (7.5), (7.8) and (7.9) are different from the GLR equation [1,2]. It is interest that the properties and structure of the simplified low- x form (7.14) is similar to a modified GLR equation that has been obtained earlier in ref. [15]. However, two equations really have a different theoretical basis. The GLR equation and its modified form are based upon the AGK cutting rules. They sum three kinds of diagrams: cutting two-ladders, one-ladder and zero-ladder, respectively. The first (see fig. 1a) is identical with our figs. 5a,b, however, the cut lines in the latter two figures (figs. 1b,c) break parton recombination and these processes should be inhibited.

In conclusion, parton recombination via QCD evolution equation is investigated using perturbative theory without the AGK cutting rules. The contributions from different cut and interference diagrams are summed and infrared safeness and momentum conservation are established. Time ordered perturbation theory is developed to establish the connections among different cut diagrams. As a consequence, a new nonlinear evolution equation is derived on a different basis from the GLR equation. Furthermore, this new evolution equation is more detailed in structure than the GLR equation.

Acknowledgments:

I would like to thank Jianwei Qiu for very helpful discussions and drawing my attention to reconsideration of the parton recombination in TOPT. I would also like to acknowledge

D. Indumathi and Jianhong Ruan for useful comments. This work was supported by National Natural Science Foundation of China and '95-Pandeng' Plan of China.

References

- [1] L.V. Gribov, E.M. Levin and M.G. Ryskin, Phys. Rep. 100 (1983) 1
- [2] A.H. Mueller and J. Qiu, Nucl. Phys. B268 (1986) 427
- [3] V.A. Abramovsky, J.N. Gribov and O.V. Kancheli, Sov. J. Nucl. Phys. 18 (1973) 593
- [4] G. Altarelli and G. Parisi, Nucl. Phys. B126 (1977) 298
- [5] Yu. L. Dokshitzer, Sov. Phys. JETP 46 (1977) 641
- [6] V.N. Gribov and L.N. Lipatov, Sov. J. Nucl. Phys, 15 (1972) 438, 675
- [7] G. Sterman, An introduction to quantum field theory, Cambridge, 1993
- [8] F.E. Close, J. Qiu and R.G. Roberts, Phys. Rev D40 (1989) 2820.
- [9] J.C. Collins, D.E. Soper and G. Sterman, in Perturbative Quantum Chromodynamics, edited by A.H. Mueller (World Scientific, Singapore) (1989) 1
- [10] J.C. Collins and D.E. Soper, Nucl. Phys. B194 (1982) 445
- [11] J.C. Collins and J.W. Qiu, Phys. Rev. D39 (1989) 1398
- [12] A.P. Bukhvostov, G.V. Frolov, L.N. Lipatov and E.A. Kuraev, Nucl. Phys. B258 (1985) 601
- [13] R.L. Jaffe, Nucl. Phys. B229 (1983) 205;
- [14] Jianwei Qiu and G. Sterman, Nucl. Phys. B353 (1991) 105; *ibid.* B 353 (1991) 137
- [15] W. Zhu, D. Xue, K. Chai and Z. Xu, Phys. Lett. B317 (1993) 200; W. Zhu, K.M. Chai and B. He, Nucl. Phys. B427 (1994) 525.

Figure Captions

Fig. 1 Two expressions of the GLR equation based on the AGK cutting rules: (left) cut vertex theory and (right) time-ordered perturbation theory; where the cuts through (a) two-, (b) one- and (c) zero-ladders, respectively.

Fig. 2 The amplitudes (a) $M_{p\gamma^* \rightarrow k'l'X}^{(2-1)}$, (b) $M_{p\gamma^* \rightarrow k'l'X}^{(2-2)}$ and (c) $M_{p\gamma^* \rightarrow k'l'X}^{(2-3)}$. The dark circles denote the PQCD interaction with the correlation of the initial partons.

Fig. 3 Naive parton model of DIS.

Fig. 4 The leading order splitting processes in DIS.

Fig. 5 The diagrams contributing to the leading recombination order from $|M_{p\gamma^* \rightarrow k'l'X}^{(2-2)}|^2$.

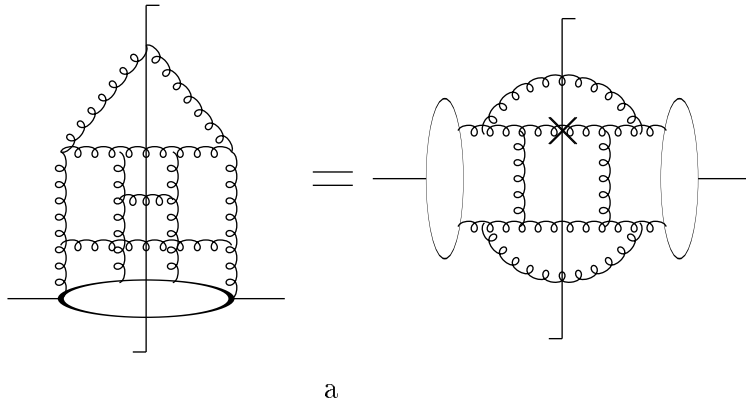
Fig. 6 Identical hadronic parts in different cut graphs from refs.[13,14].

Fig. 7 The diagrams contributing to the leading recombination order from $2M_{p\gamma^* \rightarrow k'l'X}^{(2-1)}[M_{p\gamma^* \rightarrow k'l'X}^{(2-3)}]^*$.

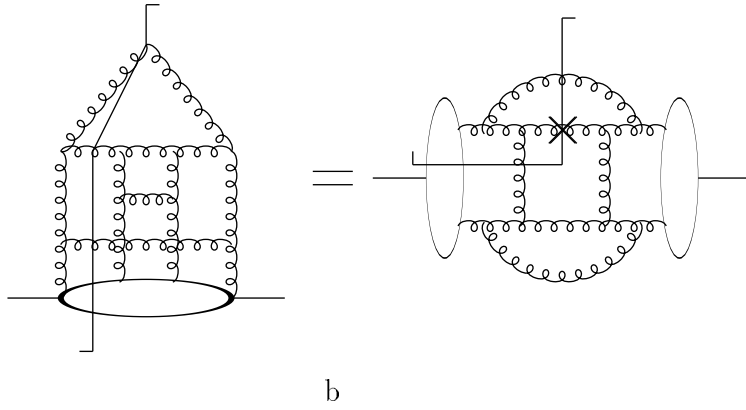
Fig. 8 A diagrammatic illustration of the relation between $P_4^{(2-2)}$ and $P_4^{(1-3)}$.

Fig. 9 A diagrammatic illustration of the time reversal invariance in $\gamma p \rightarrow \gamma p$.

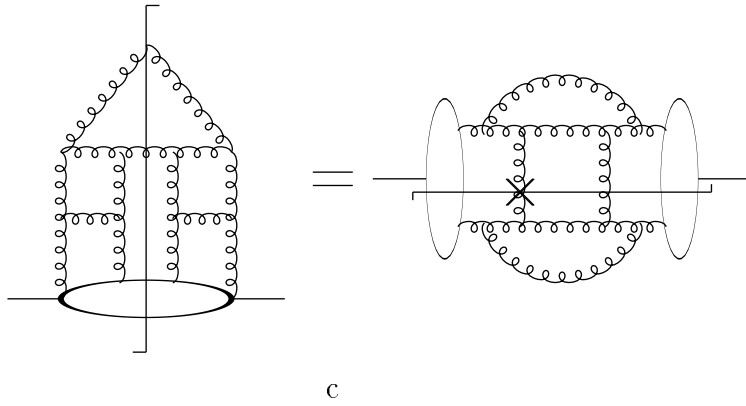
Fig. 10 IR safeness in $GG \rightarrow GG$.



a

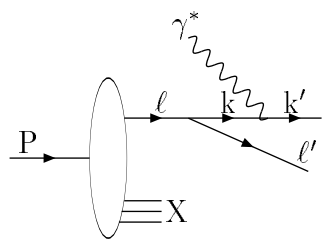


b

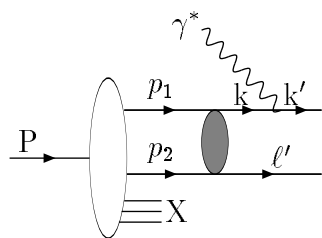


c

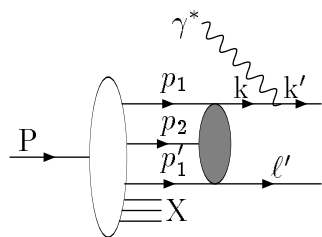
Fig.1



a

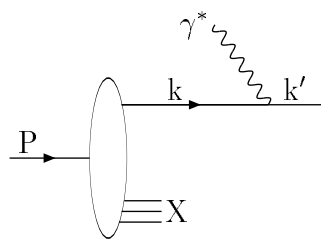


b

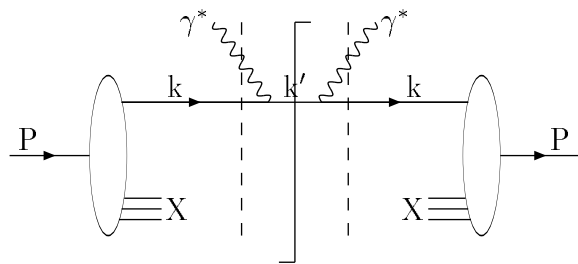


c

Fig.2



a



b

Fig.3

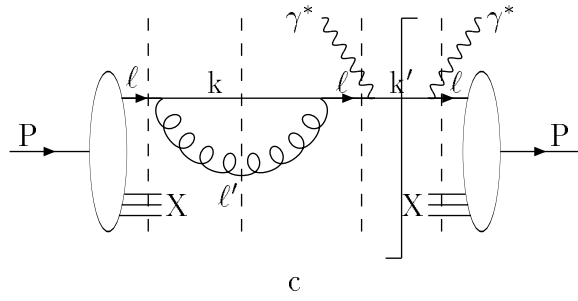
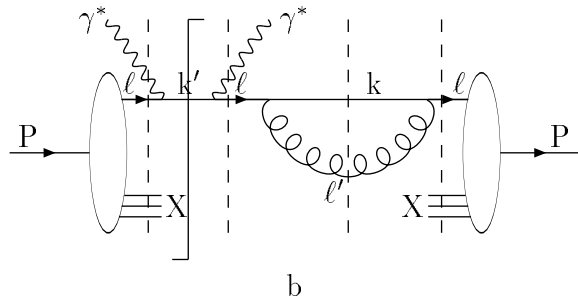
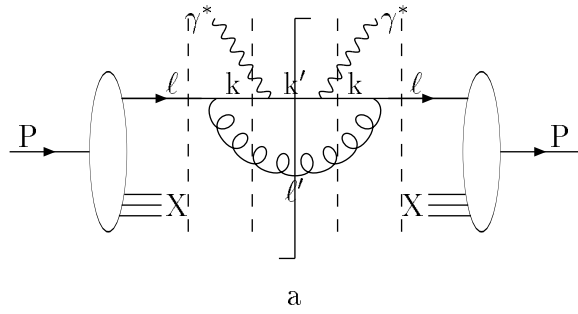


Fig.4

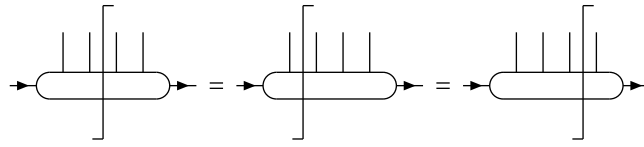
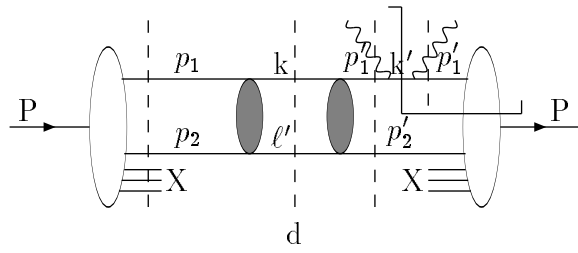
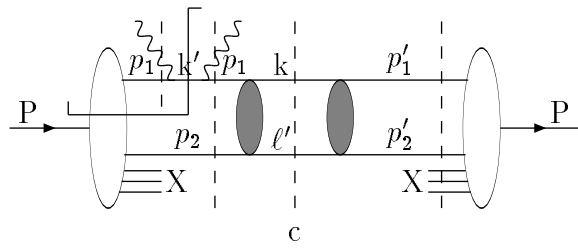
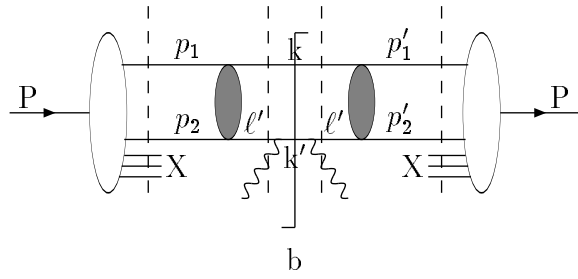
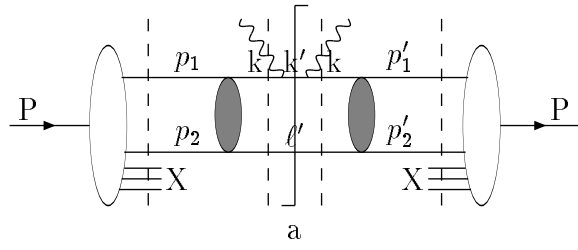


Fig.5



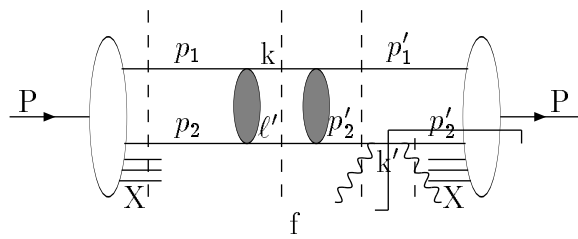
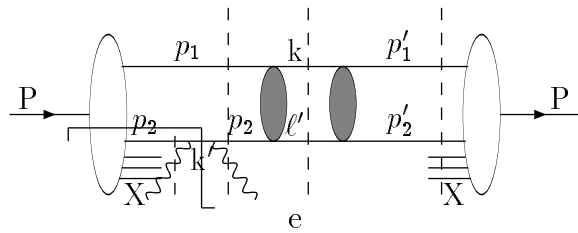
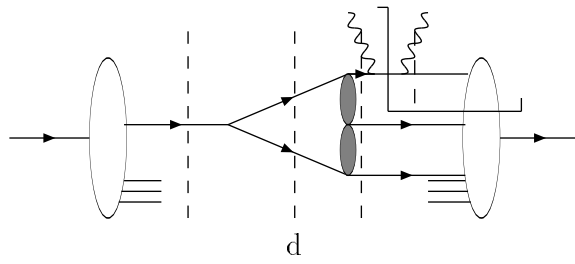
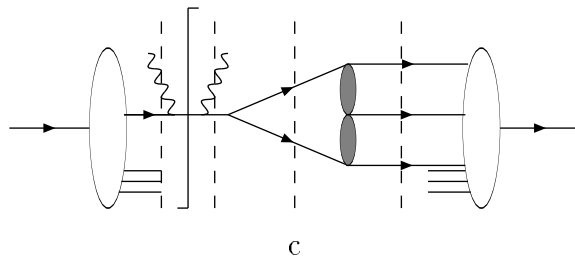
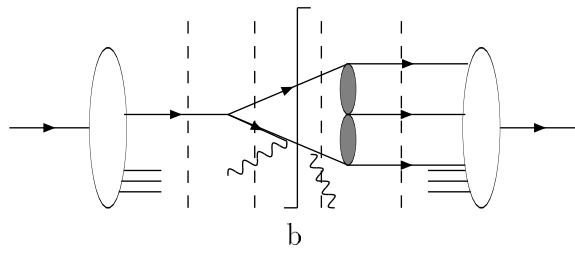
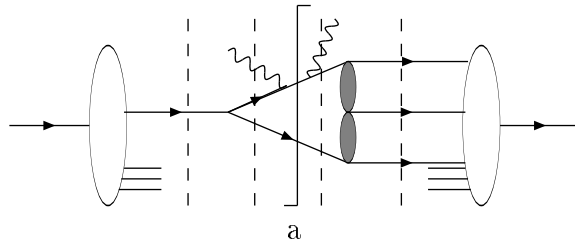


Fig.6



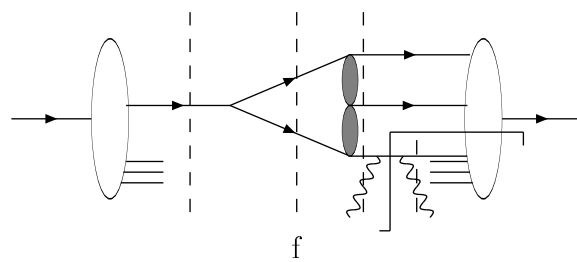
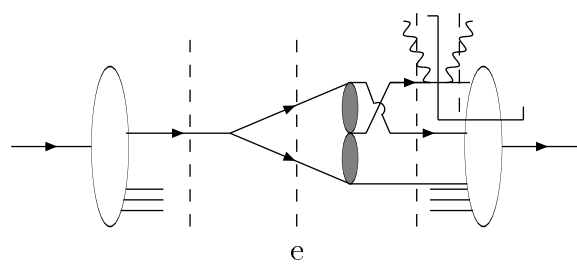


Fig.7

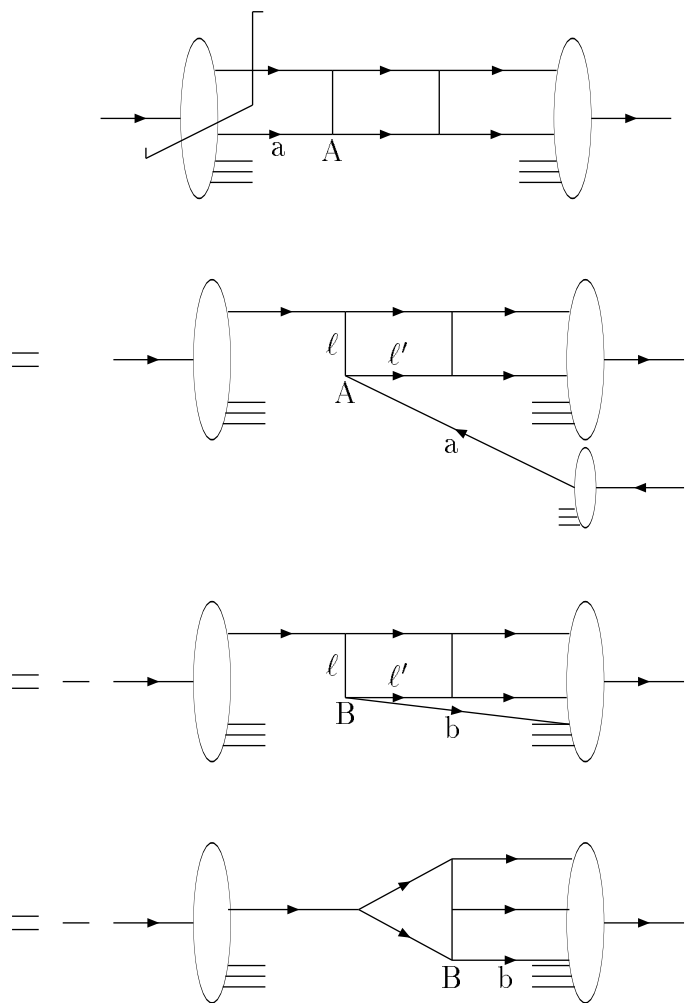


Fig.8

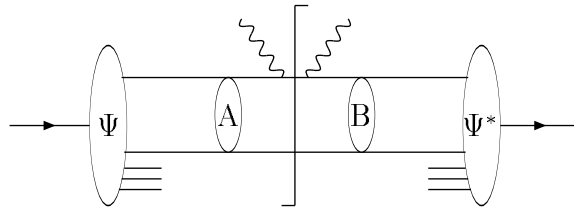


Fig.9

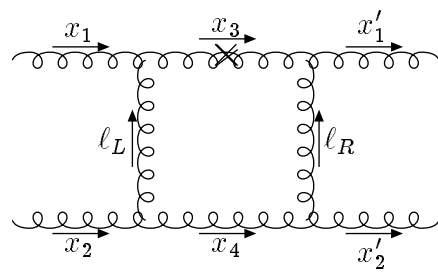


Fig.10